

Full length article

Similarity laws of geometric distortion for stiffened plate under low velocity impact loads

Xinzhe Chang ^{a,b}, Fei Xu ^{a,b,*}, Wei Feng ^{a,b}, Xiaocheng Li ^c, Xiaochuan Liu ^c^a School of Aeronautics, Northwestern Polytechnical University, Xi'an 710072, Shaanxi, China^b Institute for Computational Mechanics and Its Applications, Northwestern Polytechnical University, Xi'an 710072, Shaanxi, China^c Aviation Key Laboratory of Science and Technology on Structures Impact Dynamics, Aircraft Strength Research Institute of China, Xi'an 710065, Shaanxi, China

ARTICLE INFO

ABSTRACT

Keywords:
 Stiffened plate
 Geometric distortion
 Similarity laws
 Low velocity impact

As a thin-walled structure, it is impractical or uneconomical to scale the thickness of stiffened plate with the same scale factor as the length, which leads to geometric distortion and the failure of traditional similarity laws. In this study, firstly, the common stiffened plate structure in engineering is selected as the object, and a reasonable equivalent technique for transforming stiffened plate into double-plate structure is proposed, which is named relative plastic capacity equivalence. Then, based on the ODLV system, the similarity law of geometric distortion for beam/plate structure is compared, and the Zhao's response number of stiffened plate is derived, from which the similarity law of co-direction geometric distortion for stiffened plate is obtained expanding the object of single thin-walled plates for the ODLV system. The similarity law of hetero-direction geometric distortion for the stiffened plate structure is derived under the premise that the relative plastic capacity K of stiffeners would be constant between the scaled model and the prototype. Satisfying this premise, the yield stress of the stiffener material and the number of stiffeners along x and y directions in the plane can both be adjusted. The similarity laws of co-direction and hetero-direction geometric distortion for stiffened plates are numerically validated through several mass-impacted stiffened plates. The results show that the similarity laws can enable the geometrically distorted stiffened plate model to predict the dynamic responses of the prototype structure, such as displacement, velocity, energy and impact force.

1. Introduction

Reasonable arrangement of stiffeners is one of the common metal plate reinforcement methods, which can significantly enhance the strength characteristics of the structure. Due to the stiffened plates having their unique advantages compared with plates, they are favored in aerospace, ships and other fields, which can not only meet the required strength characteristics but also greatly reduce the weight of the structure [1–6]. In these large engineering fields, the dynamic response of structures which are subject to impact loads has received a lot of attention since long time ago. In order to investigate the dynamic response of structures under impact loads, small-scaled model tests are widely employed in large engineering structures because of their advantages such as convenient implementation, low cost and short duration [7–10]. As long as the small-scaled model meeting certain similarity conditions is designed according to the full-size prototype structure, the response of the full-size prototype structure can be predicted by the

response of the small-scaled model with the help of the similarity law [8, 9].

In the past 30 years, some scholars have studied the theoretical derivation of structural similarity theories under impact load and the specific application of scaled model in impact problems. In 1989, Jones [11] summarized the current development of similarity theories in the field of structural impact, and proposed a classical MLT (mass M- length L- time T) dimensional system that established proportional similarity laws for impacted structures. Although traditional impact similarity laws have been successful in theory and application, inherent distortion problems hinder their development because of the inability to proportionally scale physical quantities. It is crucial that the prevalence of non-similar cases exceeded that of similar ones, owing to the experimental challenges associated with producing scaled models where materials, geometric dimensions and other factors are frequently constrained [12].

Common non-similar issues may involve material strain rate effect

* Correspondence author.

E-mail address: xufei@nwpu.edu.cn (F. Xu).

(different strain rates between scaled models and prototype), different materials (different materials employed for scale models and prototype), geometric distortion (non-equal scaling in different spatial directions), and other factors [13–15]. Aiming at the no-similarity caused by strain rate effect of materials, in 2004, Oshiro and Alves [16], taking initial impact velocity V , yield stress σ_d and impact mass G as basic quantities, proposed a new set of dimensionless numbers (initial impact velocity V -yield stress S - impact mass G VSG dimensionless system) to solve this problem by adjusting the velocity scaling factor. Furthermore, Alves and Oshiro [17] developed a new method that changed the impact mass G instead of the initial velocity. In recent years, Sadeghi et al. [18–20] proposed a new type of finite similitude theory based on a set of differential equations of continuum problems. By adjusting the impact velocity of the scaled model, the problem that scaled model made of strain rate-sensitive material is not similar to the prototype under high velocity impact load is corrected.

Aiming at the no-similarity caused by different materials, which mainly involves the key physical quantities of density and yield stress for different materials, Alves and Oshiro [21] compensated for the distortion of different materials with different strain rate effects by correcting the impact velocity. Later, Mazzariol et al. [22,23] introduced the density scaling factor, corrected the impact velocity and mass of the scaled model, and verified the effectiveness of this method through experiments and finite element models. Wang and Xu [24] proposed a new DLV (density D- length L- initial impact velocity V) dimensional analysis system with concise and clear dimensionless numbers that directly relate to each physical quantity. In 2021, based on the DLV dimensional system, a new dimensionless material number M_n [25] was further proposed. By selecting appropriate similar materials, the scaled model could perfectly predict the response of the prototype structure. Through these studies, it is evident that the development of similarity theory and scaled model test has yielded fruitful results in researching correction methods for distortion caused by strain rate effect and different materials.

In practical engineering applications, the thickness direction of the thin-walled structure cannot be scaled with the in-plane dimension using the same geometric scale factor, which forms a geometric distortion model, making the traditional pure geometric similarity law invalid [26–29]. In 2005, Cho et al. [30] studied scaled models with geometric distortion and different materials, and corrected them to be associated with the prototype. In 2012, Oshiro and Alves [31] addressed the issue of geometric distortion between scaled models and prototypes made of the same material by intentionally distorting the geometric dimensions of model with thickness and the rest of the dimensions not equally scaled. The influence of geometric distortion on similarity is solved by iteratively correcting the impact velocity. Kong et al. [32] confirmed the effectiveness of the method through experiments and simulations. Mazzariol et al. [33] developed VSM (Velocity-Stress-Mass) dimensional system, and proposed dimensionless numbers that can directly reflect geometric distortion for beam and plate structures. Wang and Xu [12] also proposed a quantifiable directional ODLV (O stands for oriented) dimensional system on the basis of DLV dimensional system, and decomposed the characteristic dimension L of the structure into three vector dimensions. Although the corrected similarity method of geometric distortion has achieved significant progress, it has mainly focused on beam/plate or thin shell structures.

The stiffened plate also belongs to a thin-walled structure and faces the challenge of geometric distortion in similarity studies. In recent years, with the development of similarity theory, more and more scholars have begun to study geometric distortion similarity methods of stiffened plates [34–38], but these methods mainly focus on buckling under compressive load to ensure the similarity of key parameters during buckling. For the similar study of geometric distortion of the impacted stiffened plate, Kong et al. [39] proposed a corrected similarity relation using a scaled model in which both the plate thickness and stiffener configuration are distorted. However, this approach requires

indirection to correct the similarity relation, and this similarity relation is not able to give a definite similarity law as it changes with different geometric dimension scale factors. Under the VSG system, Zhou et al. [40] added the scale factor β_S of the static moment for plates cross-sections in order to reflect the influence of geometric distortion, and a similarity method for correcting the velocity scale factor $\beta_V = \sqrt{\beta_{\sigma_d} \beta_S / \beta_M}$ is proposed. However, this method solely takes into account the plate structure during geometric distortion scaling, disregarding the influence of stiffeners on similarity.

The fact is that it is necessary to adjust the dimensions of the stiffeners in the stiffened plate, specifically their width and height, in accordance with certain similarity conditions. Additionally, in certain instances of stiffened plates, adjusting the dimensions of the stiffeners alone may not be sufficient to solve the distortion issue, and will additionally cause the stiffener width scale factor to be excessively large, thus adjusting the number and material of the stiffeners also needs to be considered. These potential distortion cases above constitute the main content and the focused problem to be discussed in this research. The main advantage of this paper, in comparison with previous studies, lies in the extension of the object from a single beam/plate structure to a stiffened plate structure, and proposed similarity law effectively addresses the geometric distortion for both plates and stiffeners with consideration of potential distortion cases that may be faced.

In what follows, Section 2 introduces a directional framework for geometric distortion similarity law. Section 3 studies the similarity law of the co-directional geometric distortion and hetero-directional geometric distortion of stiffened plates. Section 4 investigates the numerical modeling of a stiffened plate subjected to mass impact and verifies the effectiveness of the similarity laws. Section 5 summarizes the work of this paper.

2. A review of present directional scaled framework for geometrically distorted

In this section, the current geometric distortion directional dimensionless system is reviewed, its derivation is described briefly, and the dilemmas of its application to stiffened plates are pointed out, which is also the main focus of this present study.

2.1. DLV dimensionless number system

In the structural impact similarity study, depending on the selected basic quantities, it is usually divided into three commonly used dimensional systems, namely MLT, VSG and DLV. Compared with other dimensional analysis systems, the dimensionless number of the DLV dimensional system is relatively simple and clear [24]. Therefore, the DLV dimensional system is used to derive the scaling factor of the pure geometric scaling of the structure.

For the rigid-perfectly plastic materials, the material constitutive equation has only one parameter, yield stress σ_d . With density ρ , length L and velocity V as the basic quantities, the key response variables of the structural impact, i.e., displacement δ , acceleration A , stress σ , strain ε , force F , velocity V , time t , energy E_K , structural mass M , impact mass G , are determined by Buckingham II-Theorem [41] combined with the basic equation. The following main dimensionless numbers can be obtained:

$$\left\{ \begin{array}{l} \underbrace{\left[\frac{\rho V^2}{\sigma_d} \right]}_{\Pi_1} \underbrace{\left[\frac{tV}{L} \right]}_{\Pi_2} \underbrace{\left[\frac{\delta}{L} \right]}_{\Pi_3} \underbrace{\left[\frac{M}{\rho L^3} \right]}_{\Pi_4} \underbrace{\left[\frac{AL}{V^2} \right]}_{\Pi_5} \\ \underbrace{\left[\frac{E_K}{\rho L^3 V^2} \right]}_{\Pi_6} \underbrace{\left[\frac{F}{\rho L^2 V^2} \right]}_{\Pi_7} \underbrace{\left[\frac{\dot{\varepsilon}L}{V} \right]}_{\Pi_8} \underbrace{\left[\frac{\varepsilon}{\sigma_d} \right]}_{\Pi_9} \underbrace{\left[\frac{\sigma}{\sigma_d} \right]}_{\Pi_{10}} \end{array} \right\} \quad (1)$$

2.2. Directional scaled framework (ODLV system) of geometrically distorted

It is evident from the above analysis that $\Pi_1 = \frac{\rho V^2}{\sigma_d}$ is similar to the Damage Number $D_n = \frac{\rho V^2}{\sigma_d}$ given by Johnson [42,43]. In order to compare the response for structures with different geometric dimensions, based on the damaged number D_n , Zhao [44,45] proposed a new dimensionless number for dynamic plastic response of rigid-perfectly plastic material structure, namely, Zhao's response number (abbreviated as $R_n(n)$), which is generally expressed as:

$$R_n(n) = \frac{\rho V^2}{\sigma_d} \left(\frac{L}{H} \right)^n = D_n \left(\frac{L}{H} \right)^n \quad (2)$$

In the formula, ρ is the density, V is the impact velocity of the structure, σ_d is the yield stress of the material, L and H are the two characteristic dimensions of the structure, respectively. L is always significantly greater than H , for instance, L can be taken as half the span of the beam, radius of the circular plate or half the width of the rectangular plate, and H can be taken as the thickness of the beam or plate. n is a positive real number, and different values can be taken for different structures, for a beam or a plate, $n = 2$ [12]; for the thin-walled cylindrical shell under axial impact, $n = 1/2$ [26]; for a thin-walled square tube under axial impact, $n = 2/3$ [27], as for the value of n for stiffened plate will be derived in detail in Section 3.2.

It can be seen from the expression of the response number that the characteristic dimensions of the structure will no longer belong to the same characteristic dimension. For isotropic materials, there is the same characteristic dimension L in the X-Y plane, while the characteristic length L and the characteristic thickness H are independent of each other and have the orientation. When this dimensionless number is employed to the similarity study, the thickness H of the structure will not have to be scaled according to the same geometric scaling factor with the remaining dimensions of the structure. Then, the dimensionless number proposed in Section 2.1 is corrected by combining it with Zhao's response number. The dimensionless number of stress can be re-expressed by using Zhao's response number as:

$$\Pi_1 = \frac{\rho V^2}{\sigma_d} \left(\frac{L}{H} \right)^n \quad (3)$$

It is assumed that the dimensionless number forms of stress, strain and strain rate are identical and have the same geometric power number. That is to say, the dimensionless number of strain and the dimensionless number of strain rate will become:

$$\begin{aligned} \Pi_9 &= \varepsilon \left(\frac{L}{H} \right)^n \\ \Pi_8 &= \dot{\varepsilon} H \left(\frac{L}{H} \right)^n \end{aligned} \quad (4)$$

At this time, when the geometric distortion of the structure occurs, if the displacement response direction of the structure is consistent with the thickness direction, the dimensionless number of the structure will become:

$$\left\{ \begin{array}{c} \underbrace{\left[\frac{\rho V^2}{\sigma_d} \left(\frac{L}{H} \right)^n \right]}_{\Pi_1} \underbrace{\left[tV \right]}_{\Pi_2} \underbrace{\left[\delta \right]}_{\Pi_3} \underbrace{\left[M \right]}_{\Pi_4} \underbrace{\left[AH \right]}_{\Pi_5} \\ \underbrace{\left[E_K \right]}_{\Pi_6} \underbrace{\left[F \right]}_{\Pi_7} \underbrace{\left[\dot{\varepsilon} H \left(\frac{L}{H} \right)^n \right]}_{\Pi_8} \underbrace{\left[\varepsilon \left(\frac{L}{H} \right)^n \right]}_{\Pi_9} \underbrace{\left[\sigma \right]}_{\Pi_{10}} \end{array} \right\} \quad (5)$$

Since these dimensionless numbers are associated with characteristic dimensions in different directions and are based on the DLV dimensionless system, they are termed as ODLV system [12]. According to

Buckingham Π -Theorem, the dimensionless variables between the scaled model and the prototype must be equal. For example, the equality $(\Pi_1)_m = (\Pi_1)_p$ leads to the scaling factor β_{σ_d} as $\beta_{\sigma_d} = \beta_p \beta_V^2 \left(\frac{\rho_t}{\rho_p} \right)^n$, where the subscripts m and p denote the scaled model and prototype respectively.

Similarly, other scaling factors can be derived using this way, and the scaling factors for the ODLV system of structures under impact loading can be obtained as shown in Table 1.

It can be found that by introducing Zhao's response number into the geometric distortion similarity analysis of the rigid-perfectly plastic material structure, the thickness direction and in-plane basic geometric scaling factor of the structure are separated into two independent directional factors successfully ($\beta_{L_x} = \beta_{L_y} = \beta_L$ for the isotropic rigid-perfectly plastic materials), which establishes the ODLV system. Based on the ODLV system, the geometric distortion can be solved by correcting the impact velocity, yield stress of material and density of material. Different structures have different Zhao's response numbers, in a sense, as long as the real number n of different impacted structures is obtained, the complete geometric distortion similarity law of the specific structure can be obtained from Table 1. It is worth noting that the ODLV system has the best similarity where their geometrical nonlinearity belongs to small strains, which means that the rotation angle of the neutral plane of the plate is within 10° – 15° . Thus, it is necessary to ensure that the structure is subjected to low velocity impacts.

2.3. The dilemmas of the ODLV application in stiffened plates

The ODLV system effectively overcomes the geometric non-similarities of structures on the basis of associating physical quantities with spatial characteristic dimensions. However, the ODLV system is derived based on beam/plate structures. For stiffened plates, in addition to the geometric distortion of the plates, the geometric distortion of the stiffeners is also unavoidable. This restricts the application of the ODLV system in stiffened plates.

On the whole, the geometric distortion of the stiffened plate can be classified into two types, one is co-directional geometric distortion and the other is hetero-directional geometric distortion, as shown in Fig. 1. β_H is the scale factor of plate thickness H , β_h is the scale factor of stiffener height h , and β_b is the scale factor of stiffener width b . For co-directional geometric distortion, the scale factors β_H and β_h in the same direction are no longer equal to the basic geometric scale factor β_L , and it meets $\beta_H = \beta_h \neq \beta_L$, as shown in Fig. 1a. For hetero-directional geometric distortion, the scale factors β_H and β_b in different directions are no longer equal to the basic geometric scale factor β_L , and the degree of geometric distortion between plate thickness and stiffener height is also not equal, as shown in Fig. 1b. For co-directional geometric distortion, since the stiffeners and plate have the same direction and degree of geometric distortion, the ODLV system may still be applicable. However, for hetero-directional geometric distortion, the ODLV system fails to take into account the geometric distortions of the plate and stiffeners individually and is no longer applicable.

Table 1
Scale factors for the ODLV system.

Variable	Scale factors	Variable	Scale factors
Length, L	$\beta_L = L_m/L_p$	Stress, σ	$\beta_\sigma = \beta_{\sigma_d} = \beta_p \beta_V^2 (\beta_L/\beta_H)^n$
Thickness, H	$\beta_H = H_m/H_p$	Strain, ε	$\beta_\varepsilon = (\beta_H/\beta_L)^n$
Density, ρ	$\beta_\rho = \rho_m/\rho_p$	Strain rate, $\dot{\varepsilon}$	$\beta_{\dot{\varepsilon}} = (\beta_V/\beta_H)(\beta_H/\beta_L)^n$
Velocity, V	$\beta_V = V_m/V_p$	Displacement, δ	$\beta_\delta = \beta_H$
Mass, M	$\beta_M = \beta_\rho \beta_L^2 \beta_H$	Acceleration, A	$\beta_A = \beta_V^2 / \beta_H$
Energy, E_K	$\beta_{E_K} = \beta_\rho \beta_L^2 \beta_H / \beta_V^2$	Force, F	$\beta_F = \beta_p \beta_L^2 \beta_V^2$
Impact mass, G	$\beta_G = \beta_\rho \beta_L^2 \beta_H$	Time, t	$\beta_t = \beta_H / \beta_V$

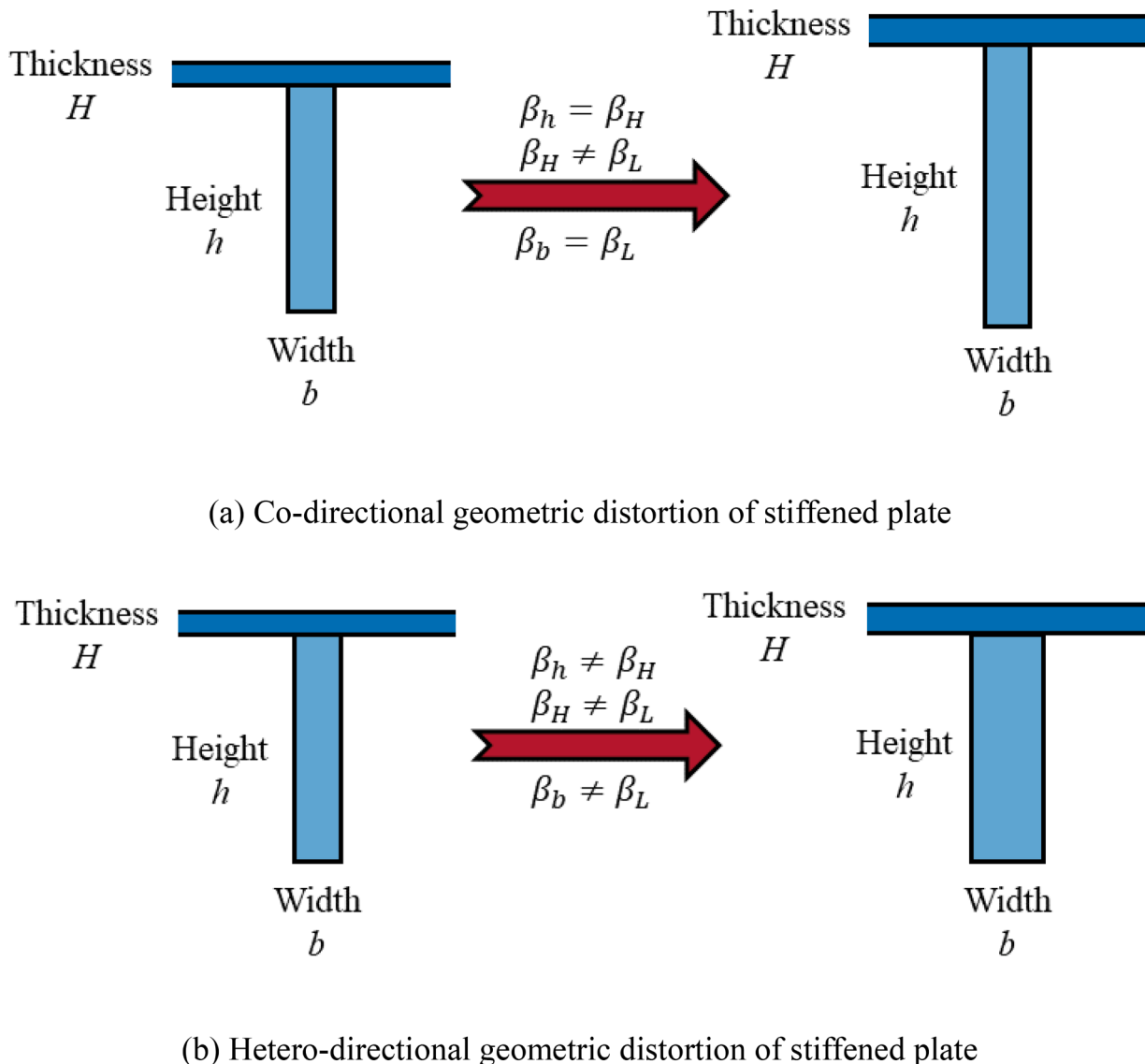


Fig. 1. Two types of geometric distortion for stiffened plates.

3. Geometric distortion similarity law of stiffened plate

In this section, a reasonable equivalent technique of the stiffened plate to a double-plate structure is presented, i.e., relative plastic capacity equivalence. And the similarity laws of co-directional geometric distortion and hetero-directional geometric distortion for stiffened plate structures are derived in detail.

3.1. Equivalent technique of stiffened plate

In recent years, numerous scholars have carried out relevant research on the dynamic response of stiffened plates under impact loads. As the

dynamic response of stiffened plate under impact loading is more intricate than that of a single beam/plate structure, numerous scholars have investigated the deformation deflection, plasticity theory and failure mode of stiffened plate by taking the stiffener equivalent to the thickness of the plate, i.e., equivalent to the double-plate structure, as shown in Fig. 2 [46–48]. The dimensions of the lower plate in the double-plate structure are consistent with that of the plate in the stiffened plate. The length and width of the upper plate are also consistent with those of the plate in the stiffened plate, while its thickness H_s is determined by the equivalent technique.

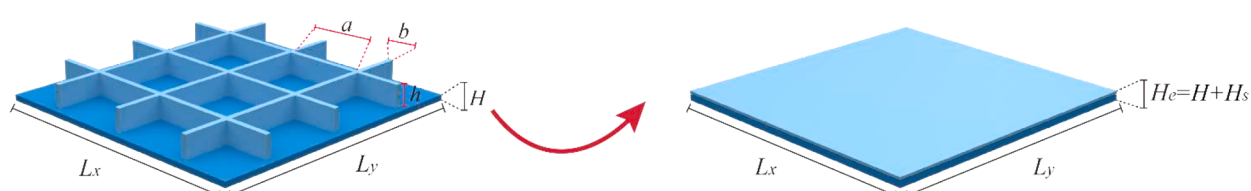


Fig. 2. Equivalent diagram of stiffened plate.

3.1.1. Equivalent technique

At present, the common equivalent techniques mainly include area equivalence (mass equivalence) and moment of inertia equivalence. In practical applications, if only moment of inertia equivalence is selected, the plate thickness will be excessively increased. If only area equivalence is chosen, the sectional moment of inertia of the stiffened plate will be lost. Therefore, in order to achieve optimal thickness equivalence of stiffeners, an equivalent technique combining area equivalence and inertia moment equivalence is proposed [47]. In addition, from the perspective of ensuring that the relative plastic capacity remains unchanged before and after the equivalence, a novel equivalent technique is proposed, namely: relative plastic capacity equivalence. The following is a detailed discussion of these equivalent techniques:

Technique I: Area equivalence (Mass equivalence)

The area of the stiffeners can be evenly distributed directly to the plate to form a double-plate structure with the same length and width [46,48]. The equivalent thickness H_e is:

$$H_e = H + H_{SI} = H + \sum \frac{A_i}{L_x} + \sum \frac{A_j}{L_y} \quad (6)$$

In the formula, A_i and A_j represent the transverse and longitudinal section area of the stiffener, respectively; H represents the thickness of stiffened plate; L_x and L_y represent the length and width of the stiffened plate, respectively.

Technique II: Comprehensive area equivalence and moment of inertia equivalence

The equivalent thickness of the stiffened plate is:

$$H_e = H + H_{SI} = H + \frac{1}{2} \left(\sqrt[3]{12I/a} + H_{SI} \right) \quad (7)$$

In the formula, I represents the moment of inertia of the stiffener; a represents the distance between stiffeners.

Technique III: Relative plastic capacity equivalence

Assuming that the dynamic yield stress of the stiffened plate material is σ_d , the width of the stiffener is b , and the height is h , the plastic ultimate bending moment of the strip plate and the plastic ultimate bending moment of the stiffener can be derived.

Plastic ultimate bending moment of strip plate:

$$M_0 = \frac{1}{4} \sigma_d H^2 a \quad (8)$$

Plastic ultimate bending moment of stiffeners:

$$M_s = \frac{1}{4} \sigma_d h^2 b \quad (9)$$

From Eqs. (8) and (9), the relative plastic capacity K of can be defined as [49,50]:

$$K = \frac{M_s}{M_0} = \frac{bh^2}{aH^2} \quad (10)$$

Under the condition that the relative plastic capacity is constant, the equivalent thickness H_e can be obtained:

$$H_e = H + H_{III} = H + \sqrt{\frac{bh^2}{a}} = H + \sqrt{KH^2} \quad (11)$$

Although the equivalent technique is investigated by taking the rectangular cross-section of the stiffeners as an example. The equivalent technique proposed for stiffened plates is not restricted by the configuration of the stiffened plate, and it is applicable to both ribbed plates with local stiffeners and integral stiffened plates. In addition, the equivalent technique is also applicable to different cross-sectional shapes of stiffeners, such as U-shaped, T-shaped, and so on. In short, it is simply necessary to ensure that the ratio of the plastic ultimate bending moment of the stiffeners and the plate remains unchanged after equivalence.

Comparing the three equivalent techniques, it is not difficult to find

that the H_{SI} and H_{II} of technique I and II are only related to the dimensions of the stiffener, while the H_{III} of technique III is not only related to the dimensions of the stiffener, but also to the thickness of the plate, that is, $H_{III} = f(H)$. In this case, if the thickness of the stiffened plate is geometric distorted, only technique III can successfully relate the thickness of the plate to the dimensions of stiffener, providing the possibility for reasonable adjustment of the dimensions of the stiffener to achieve the similarity.

3.1.2. Numerical simulation of the three equivalent techniques

(I) Finite element model

In order to compare the accuracy of different equivalent techniques for the stiffened plate equivalent to the double-plate structure in Section 3.1.1, the dynamic response is compared and analyzed before and after the equivalent, respectively. The ABAQUS software is used to establish the stiffened plate model which is common in engineering as shown in Fig. 3. The length L_x and width L_y of the stiffened plate are 600 mm, the thickness H of the plate is 2 mm, the height h and width b of the stiffener are 20 mm and 4 mm, respectively, and the distance a between the stiffeners is 150 mm. The stiffened plate is made of AL2024-T351 material, and the ideal elastic-plastic constitutive model is used for simulation analysis, material properties are shown in Table 2 [51,52].

The stiffened plate is modeled using C3D8R solid elements and the mesh number in the direction of stiffener height and plate thickness is 4, while the remaining mesh dimensions are 3 mm. The upper surface of the stiffened plate is subjected to a linear attenuation load, as shown in Fig. 4, while both the plate and stiffeners of all four sides are fully clamped. According to the geometric dimensions of the stiffened plate, the equivalent thickness of the stiffened plate with different equivalent techniques is obtained by Eqs. (6), (7) and (11). Therefore, the corresponding double-plate structure has been established in the ABAQUS software. Additionally, all remaining boundary conditions, load forms and mesh attributes are kept consistent with those of the stiffened plate. The finite element models of both the stiffened plate and double plate structure are presented in Fig. 5.

Fig. 6 presents a comparison of the dynamic response between the double-plate structure and the stiffened plate structure, which are obtained through different equivalent techniques after making the stiffened plate structure equivalent to the double-plate structure. Fig. 6a is the displacement-time response curve of the center point of the structure, Fig. 6b is the kinetic energy-time response curve of the structure, and Fig. 6c is the plastic dissipation energy-time response curve of the structure. From the dynamic response time curves of these three physical quantities, for the displacement, the error of the relative plastic capacity equivalent technique is the smallest, and the equivalent effect is the best. For kinetic energy, the error of comprehensive area equivalent and inertia moment equivalent is the smallest. For plastic dissipation energy, the error of area equivalent technique is the smallest. Therefore, different response physical quantities have different optimal equivalence techniques, and in the actual research process, the deformation deflection of stiffened plate, namely displacement, is more concerned by scholars.

In light of this, this research selects the best equivalent technique from the perspective of displacement, and further analyzes the relative error of the peak displacement of the center point of the double-plate structure and the stiffened plate structure obtained by different equivalent techniques. As shown in Table 3, the relative error of the peak displacement of the double-plate structure obtained by the relative plastic capacity equivalent technique of the stiffeners is the smallest, indicating that the equivalent effect of this technique is the best. Therefore, in the subsequent similarity study of stiffened plates, the technique of relative plastic capacity equivalence is adopted to equivalent the stiffened plates.

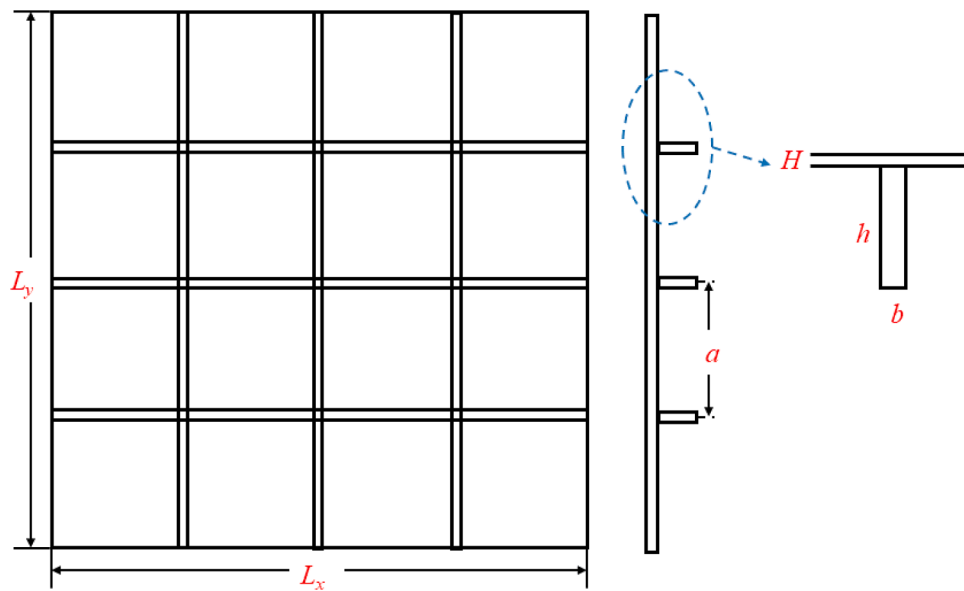


Fig. 3. Structure dimensions diagram of stiffened plate.

Table 2
Material properties.

Material	Elastic modulus E/GPa	Poisson's ratio μ	Density $\rho/[\text{g}/\text{cm}^3]$	Yield stress σ_d/MPa
AL2024-T351	71	0.3	2.70	265

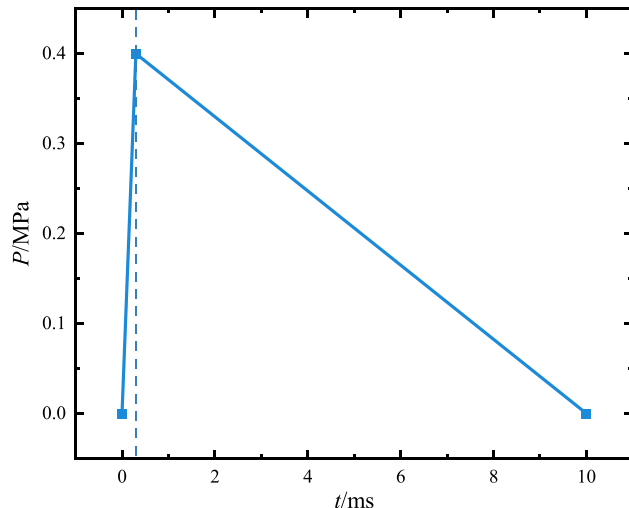


Fig. 4. Impact load curve.

3.2. Similarity law analysis of co-directional geometric distortion

The stiffened plate can be viewed as a structure consisting of a plate and stiffeners. Therefore, the similarity law of dynamic response of beam structure and plate structure under low velocity impact load is firstly derived. According to the research of Wang and Xu [12], it can be obtained that there are the same Zhao's response number for beam and plate structures under impact loading, which is as follow:

$$Rn(2) = \frac{\rho V^2}{\sigma_d} \left(\frac{L}{H} \right)^2 \quad (12)$$

Furthermore, as demonstrated in Section 2.2, and based on the ODLV

system, it can be obtained that under the low velocity impact load, the plate structure and the beam structure have the same geometric distortion scale factor as shown in Table 4, and the scaling factors of the remaining dynamic variables are consistent with those in Table 1.

Therefore, when the direction and degree of geometric distortion between beams and plates are the same, after the beam and plate are combined to form a stiffened plate, the stiffened plate should have the same geometric distortion scale factors as those of the beam and the plate.

In addition, in the definition of Zhao's response number R_n as outlined in Section 2.2, the equivalent thickness of the stiffened plate is used to replace the thickness of the single plate. Then, combined with Eq. (12), the Zhao's response number R_n of the stiffened plate can be proposed as:

$$Rn(2) = \frac{\rho V^2}{\sigma_d} \left(\frac{L}{H_e} \right)^2 \quad (13)$$

Based on the aforementioned analysis, the scale factors of co-directional geometric distortion of stiffened plate under low velocity impact load can be obtained as shown in Table 5, and the scaling factors pertaining to the remaining dynamic variables conform with those presented in Table 1.

3.3. Similarity law analysis of hetero-directional geometric distortion

The common stiffened plate structure shown in Fig. 3 is selected as the object. In analyzing the effect of impact load intensity on the failure mode of the stiffened plate, Hou [53] proposed a dimensionless impact load Φ that takes into account both the structural geometric dimensions of stiffened plates and the form of impact loads:

$$\Phi = \frac{QL_y}{H_e^2 \sqrt{\rho \sigma_d}} \quad (14)$$

In the formula:

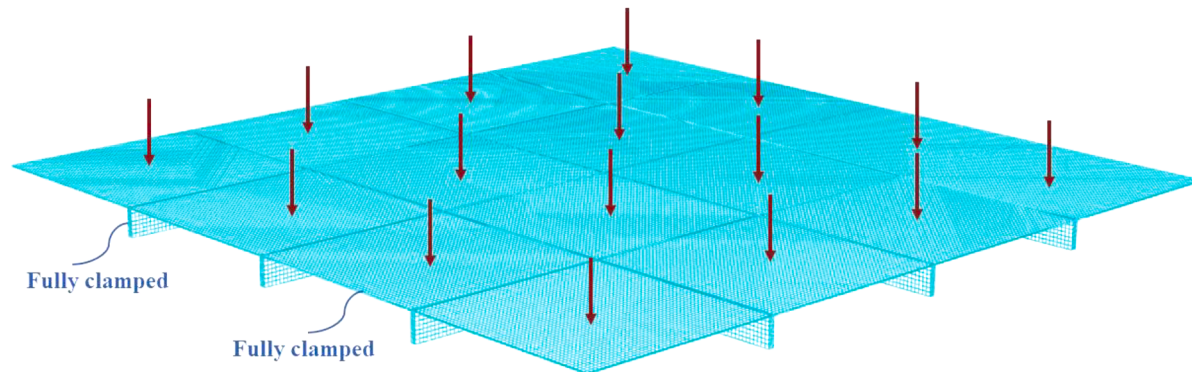
Q — Air explosion shock wave specific impulse, $\text{N}\cdot\text{s}/\text{m}^2$;

L_y — Width of the stiffened plate;

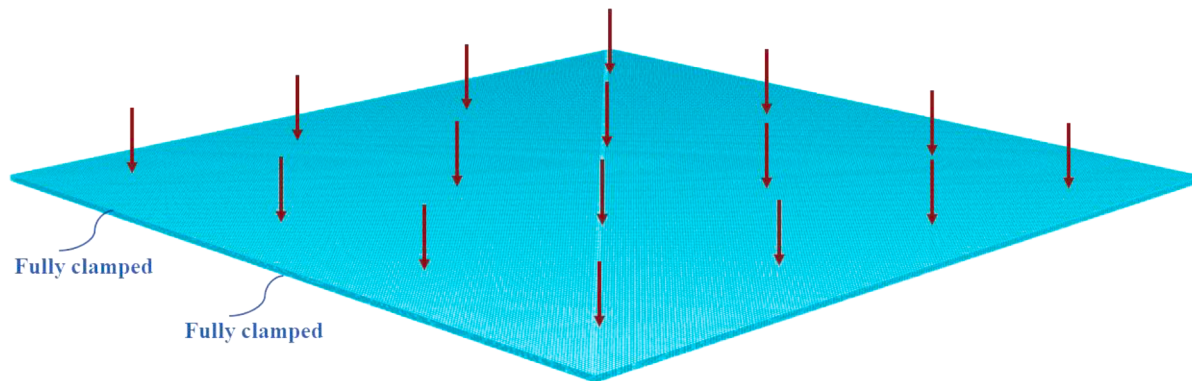
H_e — The equivalent thickness of stiffened plate obtained by the relative plastic capacity equivalent technique;

σ_d, ρ — Yield stress and density of material.

By the law of conservation of momentum, using velocity instead of impulse can be obtained:



(a) Finite element model of the stiffened plate



(b) Finite Element Model of the double-plate structure

Fig. 5. Finite element model.

$$Q = \frac{GV}{L_x L_y} \quad (15)$$

Substituting Eq. (15) into Eq. (14), we can get:

$$\Phi = \frac{\frac{GV}{L_x L_y} L_y}{H_e^2 \sqrt{\rho \sigma_d}} \quad (16)$$

The mass M of the stiffened plate is:

$$M = \rho L_x L_y H_e \quad (17)$$

Substituting Eq. (17) into Eq. (16), then Eq. (16) can be further transformed into:

$$\Phi = \frac{\frac{GV}{M} L_y \rho}{H_e \sqrt{\rho \sigma_d}} = \frac{G}{M} \sqrt{\frac{\rho V^2}{\sigma_d} \left(\frac{L_y}{H_e} \right)^2} \quad (18)$$

Similar to the simple plate structure, the stiffened plate also exhibits three primary failure modes under the impact load: Mode I: large plastic deformation; Mode II: tensile tearing at supports; Mode III: shear tear failure [54,55]. Assuming that only plastic deformation occurs in the stiffened plate (it is generally believed that D_{max} should be less than 20 [56,57]), so the stiffened plate should be subjected to low velocity impacts), and all of them are large plastic deformation, and the plastic deformation of the stiffened plate lattice is comparatively smaller than that of the entire structure, the dimensionless deflection D_{max} is [49]:

$$D_{max} = \frac{\delta_{max}}{H} \quad (19)$$

When the stiffened plate only undergoes significant plastic deformation, under the condition that the relative plastic capacity K remains constant, the dimensionless deflection D_{max} increase monotonically with the increase of the dimensionless impact load Φ . Furthermore, there exists a clear linear relationship between dimensionless deflection D_{max} and dimensionless impact load Φ [49,56,58].

It can be obtained that the relationship between the dimensionless deflection D_{max} and the dimensionless impact load Φ is $D_{max} = \lambda \Phi$, where λ is a constant coefficient that does not affect the dimensional analysis process. Furthermore, simultaneous Eqs. (18) and Eq. (19) can be derived:

$$\frac{\delta_{max}}{H} = \lambda \frac{G}{M} \sqrt{\frac{\rho V^2}{\sigma_d} \left(\frac{L_y}{H_e} \right)^2} \quad (20)$$

From the previous derivation, it is evident that in order to ensure the validity of Eq. (20), the relative plastic capacity K must remain constant. In other words, for a scaled stiffened plate structure, the relative plastic capacity K between the scaled model and prototype must satisfy certain conditions:

$$\beta_K = 1 \quad (21)$$

In addition, for Eq. (11) to satisfy similarity between scaled model and the prototype, it is also necessary to meet $\beta_K = 1$. By utilizing the equation analysis method and incorporating the definition of relative plastic capacity K as presented in Eq. (10), a scaling relationship between structural geometric dimensions of the stiffened plate can be established:

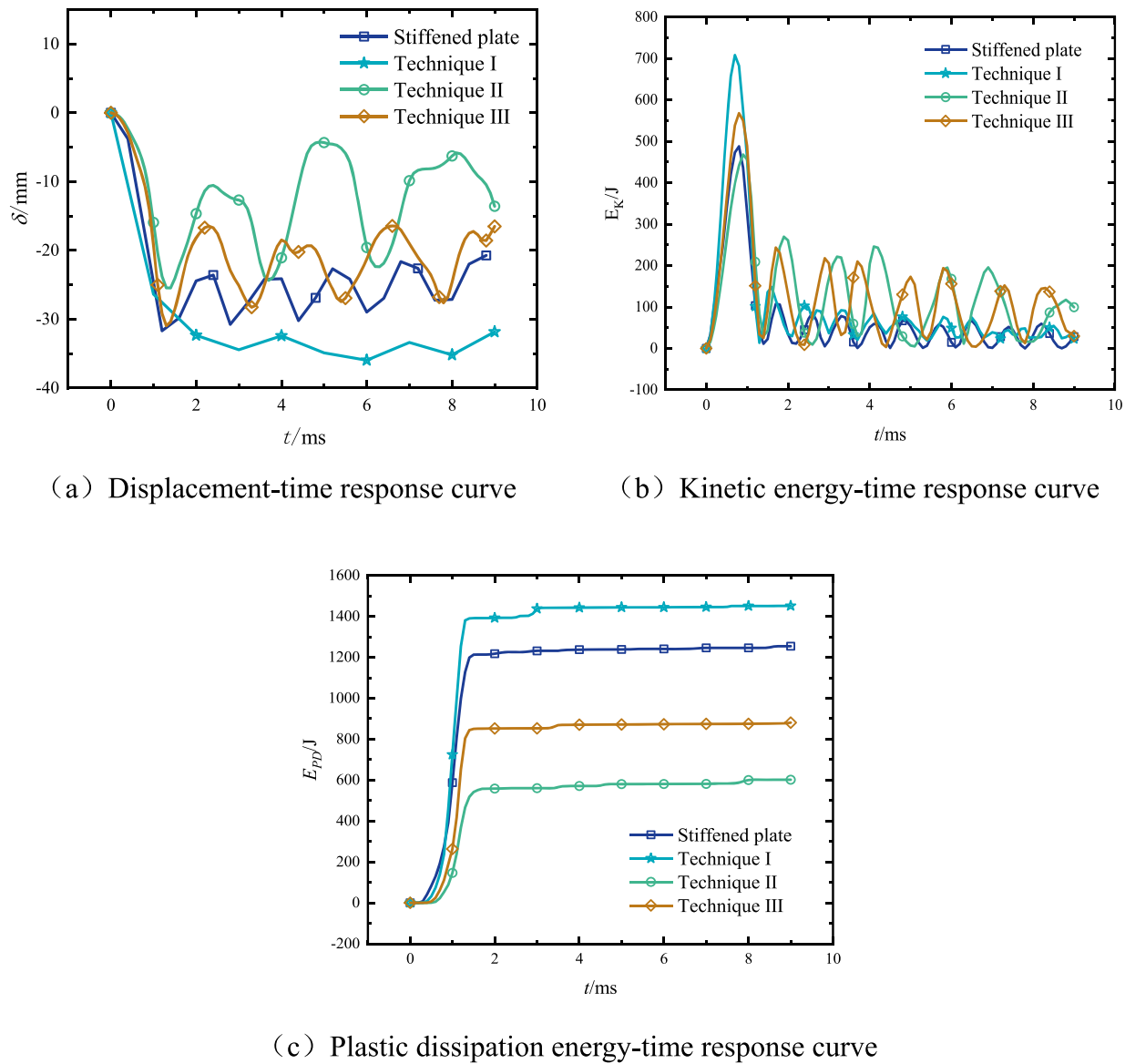


Fig. 6. Comparison of dynamic response among different equivalent techniques.

Table 3
Peak displacement error of center point under different equivalent techniques.

Equivalent techniques	Peak displacement of center point /mm	Relative error /%
Stiffened plate	31.68	/
Technique I	34.44	8.71
Technique II	25.46	19.63
Technique III	30.96	2.27

Table 4
Scale factors of geometric distortion model of beam/plate structure.

Variable	Scale factors	Variable	Scale factors
Length, L	$\beta_L = L_m/L_p$	Stress, σ	$\beta_\sigma = \beta_{a_x} = \beta_p \beta_V^2 (\beta_L/\beta_H)^2$
Thickness, H	$\beta_H = H_m/H_p$	Strain, ϵ	$\beta_\epsilon = (\beta_H/\beta_L)^2$
Displacement, δ	$\beta_\delta = \beta_H$	Strain rate, $\dot{\epsilon}$	$\beta_{\dot{\epsilon}} = (\beta_V/\beta_H)(\beta_H/\beta_L)^2$

Table 5
Scale factors of co-directional geometric distortion model of stiffened plate.

Variable	Scale factors	Variable	Scale factors
Length, L_x, L_y	$\beta_{L_x} = \beta_{L_y} = \beta_L = L_m/L_p$	Plate thickness, H	$\beta_H = H_m/H_p$
Stiffener height, h_x	$\beta_{h_x} = \beta_{h_y} = \beta_H = h_y$	Stiffener width, b_x	$\beta_{b_x} = \beta_{b_y} = b_y$
Distance, a_x, a_y	$\beta_{a_x} = \beta_{a_y} = \beta_L$		

$$\beta_b \beta_h^2 = \beta_a \beta_H^2 \quad (22)$$

In the x and y directions in the plane, the distance scale factor β_{a_x}, β_{a_y} between the stiffeners does not need to be consistent, and only needs to satisfy $\beta_K = 1$ during the scaling process. In this case, the number of stiffeners in the scaled model may not be the same as the prototype.

Through Eq. (20), three dimensionless numbers of the stiffened plate structure under low velocity impact load, namely, dimensionless displacement, dimensionless mass and dimensionless dynamic yield stress can be obtained:

$$\Pi_1 = \frac{\delta}{H}; \Pi_2 = \frac{G}{M}; \Pi_3 = \frac{\rho V^2}{\sigma_d} \left(\frac{L_y}{H} \right)^2 \quad (23)$$

Further, compared with the definition of Zhao's response number, it can be observed that the dimensionless dynamic yield stress Π_3 of Eq. (23) is equivalent to Zhao's response number of stiffened plate structure. Based on the above analysis and ODLV system in Section 2.2, the scale factor of the hetero-directional geometric distortion of stiffened plate under the low velocity impact load can be obtained as shown in Table 6, and the scaling factors pertaining to the remaining dynamic variables conform with those presented in Table 1.

4. Numerical analysis

In this section, numerical models of the mass-impacted stiffened plate for scaled models and prototypes are established to validate more details of the proposed co-directional geometric distortion and hetero-directional geometric distortion similarity laws. The validity of the similarity law is evaluated from the perspective of displacement, velocity, energy and load, and the similarity error is briefly analyzed.

4.1. Co-directional geometric distortion

4.1.1. Numerical modeling

In order to verify the ability of the co-directional geometric distortion similarity laws derived from the theoretical analysis in Section 3.2, the mass-impacted model of stiffened plate shown in Fig. 7 is established in the ABAQUS software. For the geometric dimensions of the prototype as shown in Fig. 3, $L_x = L_y = 600\text{mm}$, $H = 2\text{mm}$, $h = 20\text{mm}$, $b = 4\text{mm}$ and $a = 150\text{mm}$ are adopted, respectively. As a co-directional geometric distortion model, the height distortion of each geometric distortion model is the same as the thickness.

The prototype of the stiffened plate is made of AL2024-T351, and in order to simulate rigid-perfectly plastic material, as far as possible to eliminate the effect of elasticity, the elastic modulus is set to be one hundred times larger than the actual value, material properties are shown in Table 2. Stiffened plate is simulated by C3D8R solid element, the number of meshes in thickness direction is 4, the mass ball is simulated by discrete rigid element, and the prototype mesh dimensions is 3 mm which is obtained as presented in Appendix A. The mesh dimensions of the scaled model also need to be scaled according to the geometric scale factor. The four sides of the stiffened plate structure including plate and stiffeners are clamped boundary conditions, and the center point of the prototype is impacted by a mass ball with a radius of 20 mm, whose geometric dimension is also scaled according to the geometric scale factor. Its mass is 16 kg and initial impact velocity is 6 m/s. The friction coefficient between the stiffened plate and the ball is 0.2.

Based on the ODLV system, the geometrical distortion is compensated by correction methods for velocity, yield stress, and density, therefore the validity of these correction methods is further verified in the similarity law of co-directional distortion in stiffened plates.

Table 6
Scale factors of hetero-directional geometric distortion model of stiffened plate.

Variable	Scale factors	Variable	Scale factors
Length, L_x, L_y	$\beta_{L_x} = \beta_{L_y} = \beta_L = L_m / L_p$	Plate thickness, H	$\beta_H = H_m / H_p$
Distance, a_x	$\beta_{a_x} = (a_x)_m / (a_x)_p$	Distance, a_y	$\beta_{a_y} = (a_y)_m / (a_y)_p$
Stiffener height, h_x	$\beta_{h_x} = (h_x)_m / (h_x)_p$ $(\beta_{h_x} = \beta_L \text{ or } \beta_{h_x} \neq \beta_L)$	Stiffener height, h_y	$\beta_{h_y} = (h_y)_m / (h_y)_p$ $(\beta_{h_y} = \beta_L \text{ or } \beta_{h_y} \neq \beta_L)$
Stiffener width, b_x	$\beta_{b_x} = \beta_{a_x} \beta_H^2 / \beta_{h_x}^2$	Stiffener width, b_y	$\beta_{b_y} = \beta_{a_y} \beta_H^2 / \beta_{h_y}^2$

- Corrected velocity β_V : Distortion model I - Distortion model IV

Four geometric distortion scaled models from Distortion model I to Distortion model IV are established with basic geometric scale factor $\beta_L = 1/10$ and scale factor $\beta_H = 0.12, 0.15, 0.18$ and 0.20 in the thickness direction of the plate, respectively. Here we define the degree of geometric distortion $\eta_H = \beta_H / \beta_L$. Only the impact velocity is corrected without correcting the density and yield stress in the Distortion model I to Distortion model IV. According to the structural scaling factors shown in Table 1 and Table 5, the scale factors of the input parameters and the scale factors of the dynamic quantities of the structural response corresponding to each model at different degrees of geometric distortion can be obtained, as shown in Table 7.

- Corrected yield stress β_{σ_d} and density β_ρ : Distortion model V

In the case of geometric distortion $\eta_H = 2.0$, only the density and yield stress are corrected without correcting the impact velocity in the Distortion model V. In this case, the scaling factors for yield stress and density are calculated to be $\beta_{\sigma_d} = 0.5$ and $\beta_\rho = 2.0$, respectively, and the scaling factors for the remaining physical quantities would be the same as shown in Table 7 for Distortion model IV.

4.1.2. Results analysis

The results of the finite element numerical simulation for the geometric distortion scaled model and the prototype are presented in Fig. 8 and Fig. B1 of Appendix B. Fig. 8 shows the dynamic response curves (unscaled) before scaling of the geometric distortion scaled model and the predicted dynamic response curves of the prototype (scaled) after scaling by the response scaling factors in Table 7. Among them, Fig. 8a is the displacement-time response curve of the ball, Fig. 8b is the velocity-time response curve of the ball, Fig. 8c is the energy-time response curve of the ball, and Fig. 8d is the load time-curve. Fig. B1 presents the distribution of deformation and stress for the prototype and geometric distortion scaled models.

It can be seen from Fig. 8 that the time and value of the corresponding points on each response curve of the rigid-perfectly plastic stiffened plate scaled model with different geometric distortion degrees are inconsistent. After scaling, the curve consistency between the co-directional geometric distortion scaled model and the prototype is significantly improved.

For the key design parameter displacement δ , the correction for velocity, yield stress, and density all show that the response curve of the scaled model exhibits favorable agreement with that of the prototype during the ball falling impact process, but the coincidence degree is not very good during the ball rebound process. This is due to a certain similarity error in the peak displacement of the scaled model and the prototype. Thus, in the case of almost the same rebound velocity, the degree of coincidence between the curve and the prototype during the rebound process of the ball is not very well, but the error has been greatly reduced compared with before the correction, and the overall time trend consistency is relatively good. Therefore, the relative error of peak displacement between the scaled model and the prototype is analyzed. As shown in Table 8, even when the geometric distortion degree reaches 2, the similarity error of the peak displacement of the prototype predicted by the co-directional geometric distortion scaled model with corrected velocity, yield stress, and density all does not exceed 11 %.

In summary, when the scaling process of stiffened plate conforms to the similarity law of co-directional geometric distortion presented in Section 3.2, the dynamic response of the co-directional geometric distortion scaled model can predict that of the prototype with a certain degree of error tolerance.

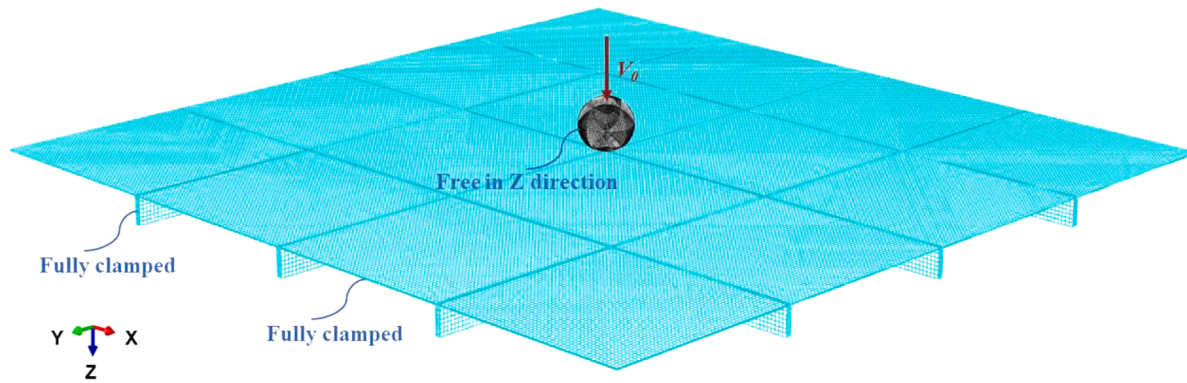


Fig. 7. Stiffened plate subjected to mass impact.

Table 7
Scale factors of the co-directional geometric distortion model.

Model	Geometric dimension and impact load					Response quantity		
	$\beta_L = \beta_b$	$\beta_h = \beta_H$ $\beta_H \neq \beta_L$	β_G	β_t	β_v	β_{E_k}	β_δ	β_F
Prototype	1	1	1	1	1	1	1	1
Distortion model I	0.1	0.12	0.0012	0.1	1.2	0.0017	0.12	0.0144
Distortion model II	0.1	0.15	0.0015	0.1	1.5	0.0034	0.15	0.0225
Distortion model III	0.1	0.18	0.0018	0.1	1.8	0.0058	0.18	0.0324
Distortion model IV	0.1	0.20	0.0020	0.1	2.0	0.0080	0.20	0.0400

4.2. Hetero-directional geometric distortion

4.2.1. Numerical modeling

In order to verify the accuracy and applicability of the hetero-directional geometric distortion similarity laws derived from the theoretical analysis of Section 3.3, the numerical model of stiffened plate under mass impact shown in Fig. 7 is established in the ABAQUS software. The geometric dimensions, materials, impacted load conditions, and so on for the prototype of the stiffened plate are the same as those in Section 4.1.1. As a hetero-directional geometric distortion model, the height distortion is not the same as the thickness distortion for each geometric distortion model.

- $\beta_{h_x} = \beta_{h_y} = \beta_L \neq \beta_H$: Distortion model I - Distortion model IV

Under the condition that the height of stiffener does not undergo geometric distortion, the distortion degree of stiffener width of each geometric distortion model can be obtained by Eq. (22). Four geometric distortion scaled models from Distortion model I to Distortion model IV are established with basic geometric scale factor $\beta_L = 1/10$ and scale factor $\beta_H = 0.12, 0.15, 0.18$ and 0.20 in the thickness direction of the plate, respectively. Compensation of geometrical distortion by correcting the velocity, according to the scale factor of hetero-directional geometric distortion model of stiffened plate under low velocity impact load given in Tables 1 and 6, the scale factors of input parameters are obtained, as shown in Table 9. Then, the scaling factors of the remaining dynamic variables of each model under different geometric distortion conditions can also be obtained, as shown in Table 9.

In addition, in the case of some stiffened plates, adjusting the dimensions of the stiffeners alone may not be sufficient to solve the distortion problem, and will also result in an excessive stiffener width scale factor, which needs to be considered for adjusting the number and material of the stiffeners. Therefore, on the basis of the Distortion model IV, three distortion models with both height and width of the stiffeners distorted, adjusting the number of stiffeners in one of the directions in the plane, and adjusting the material of the stiffeners are established to verify that the hetero-directional geometric distortion similarity laws

have the ability to carry out a flexible control of the stiffener width scaling factor.

- $\beta_{h_x} = \beta_{h_y} \neq \beta_L \neq \beta_H$: Distortion model V

In the case of geometric distortion $\eta_H = 2.0$ in the thickness direction of the plate, to verify the applicability of the similarity laws, a scaled model is established with geometric distortions in both the width and height of the stiffener. Here, $\beta_h = 0.15$ is selected and $\beta_b = 0.178$ is obtained from Eq. (22), and the scaling factors of the adjusted input parameters are shown in Table 10.

- Adjusting the number of stiffeners: Distortion model VI

In the case of geometric distortion $\eta_H = 2.0$ in the thickness direction of the plate, the geometric distortion scaled model of $\beta_{a_x} \neq \beta_{a_y}$ and $\beta_{a_x} \neq \beta_L$ is established to verify the applicability of the similarity laws. The number of stiffeners in the x and y directions of the scaled model is 2 and 3 respectively, which in turn leads to $\beta_{h_x} = 0.10, \beta_{b_x} = 0.53, \beta_{a_x} = 0.13$, and the scaling factors of the adjusted input parameters are shown in Table 10.

- Adjusting the yield stress of the stiffener material: Distortion model VII

In addition, it can be seen from Eqs. (8) and (9) that the scaled model has the possibility of different materials between the stiffeners and the plate, at which time Eq. (22) becomes $\beta_{(\sigma_d)_b} \beta_h^2 \beta_b = \beta_{(\sigma_d)_p} \beta_H^2 \beta_a$. Therefore, a scaled model with stiffeners $\beta_{(\sigma_d)_b} = 2.0$ is established for validation and can be obtained as $\beta_h = 0.10, \beta_b = 0.20, \beta_a = 0.10$, and the scaling factors of the adjusted input parameters are shown in Table 10.

The scaling factors of the remaining physical quantities for these three distortion models are the same as those in Table 9. These three distortion models comprehensively verify the similarity law of hetero-directional geometric distortion of stiffened plate, and can be adjusted with reference to these three distortion schemes if η_b is too large causing

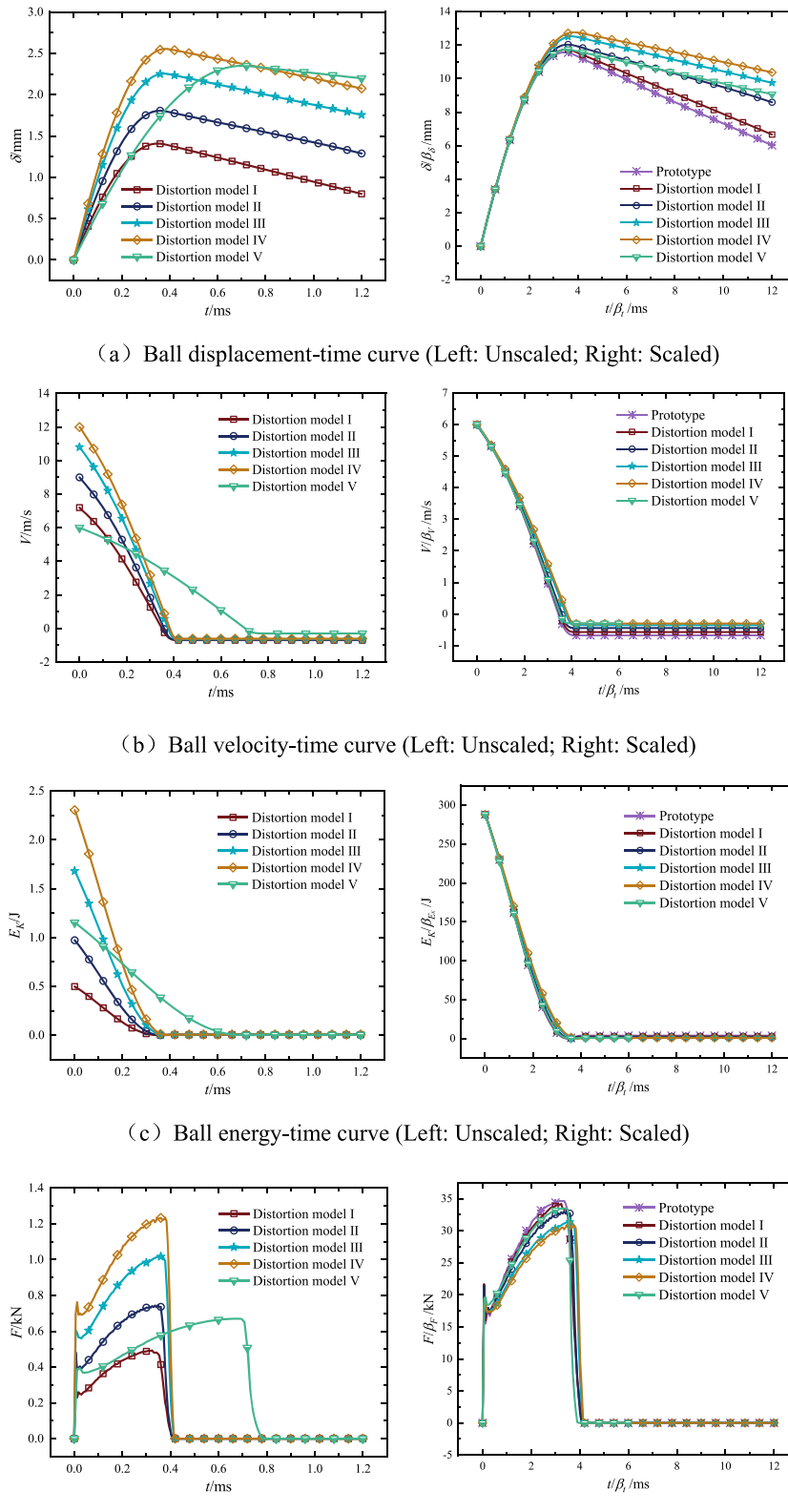


Fig. 8. Dynamic variable-time response curve of prototype and scaled model.

problems such as failure to manufacture.

4.2.2. Results analysis

The results of the finite element numerical simulation for the

geometric distortion scaled model and the prototype are presented in Fig. 9 and Fig. B2 of Appendix B. Fig. 9 shows the dynamic response curves (unscaled) before scaling of the geometric distortion scaled model and the predicted dynamic response curves of the prototype

Table 8
Similarity error of peak displacement predicted by scaled model.

Model	δ/β_δ /mm	Similarity error /%
Prototype	11.5689	/
Distortion model I	11.7319	1.409
Distortion model II	12.0386	4.060
Distortion model III	12.5242	8.257
Distortion model IV	12.7707	10.388
Distortion model V	11.7448	1.520

(scaled) after scaling by the response scaling factors in Table 9. Fig. 9a is the displacement-time response curve of the ball, Fig. 9b is the velocity-time response curve of the ball, Fig. 9c is the energy-time response curve of the ball, and Fig. 9d is the load-time curve. Fig. B2 presents the distribution of deformation and stress for the prototype and geometric distortion scaled models.

From Fig. 9, it can be seen that before scaling, the response curves of the rigid-perfectly plastic stiffened plate scaled model with different geometric distortion degrees are basically unable to coincide, and the time and value of the corresponding points on each response curve are different. After scaling, the consistency of the displacement, velocity, energy and load-time curves of the stiffened plate structure between the geometric distortion scaled model and the prototype is significantly improved.

For the two key design parameters displacement δ and load F in the derivation process of this paper, when the geometric distortion of the stiffened plate structure in different directions (i.e., only the thickness H of the plate and the width b of the stiffener, Distortion model I - Distortion model IV), the displacement and load curves of the scaled model coincide very well with the response curves of the prototype. Furthermore, the relative error of peak displacement between the scaled model and the prototype is analyzed. From Table 11, for Distortion model I - Distortion model IV, it can be seen that even when the geometric distortion degree reaches 2, the hetero-directional geometric distortion scaled model predicts the peak displacement of the prototype with a similarity error not exceeding 3 %.

When the geometric distortion of the stiffened plate structure in different directions and the height of the stiffener also has different distortion degree (i.e., Distortion model V), the displacement and load-time curves of the geometric distortion scaled model are not coincidence well with the prototype. As can be seen from Table 11, the relative error between the peak displacement predicted by the scaled model and that of the prototype is less than 7 %. This is due to the displacement-time

curve of the stiffened plate structure has a certain error when only the plate thickness and the width of the stiffener are distorted. If the height distortion of the stiffener is further superimposed, it will lead to an increased error in the displacement-time curve.

For the three distortion schemes that address the case of excessive width distortion of the stiffeners, Table 11 shows that Distortion model VI has the largest similarity error, Distortion model V has the second largest, and Distortion model VII has the smallest. This is mainly due to the change in the number of stiffeners in the Distortion model VI and the significant difference between the scaled model configuration and the prototype configuration, resulting in a poorer displacement similarity, however, the similarity error is not more than 10 %, and overall the scaled model can predict the response of the prototype.

In summary, the dynamic response of the geometric distortion scaled model can predict that of the prototype with good similarity when the scaling process of stiffened plate satisfies the similarity law of hetero-directional geometric distortion as presented in Section 3.3.

Further in the real structure, if the material constitutive model is considered bi-linear or fully nonlinear model, a similarity method called the direct scaling method can be adopted to correct the impact velocity and solve the strain rate and strain hardening effect of the material [59]. Using $(\dot{\epsilon}, \epsilon)$ represents the material constitutive model, the corrected velocity scale factor β_V^* can be obtained by the optimal approximation, as follows:

$$\| f_m \left\{ \dot{\epsilon}_p \frac{\beta_V^*}{\beta_H} \left(\frac{\beta_H}{\beta_L} \right)^2, \epsilon_p \left(\frac{\beta_H}{\beta_L} \right)^2 \right\} \frac{1}{\beta_p \beta_V^{*2}} - f_p(\dot{\epsilon}_p, \epsilon_p) \|_2 = \\ \min_{\beta_V \in R} \| f_m \left\{ \dot{\epsilon}_p \frac{\beta_V}{\beta} \left(\frac{\beta_H}{\beta_L} \right)^2, \epsilon_p \left(\frac{\beta_H}{\beta_L} \right)^2 \right\} \frac{1}{\beta_p \beta_V^2} - f_p(\dot{\epsilon}_p, \epsilon_p) \|_2.$$

5. Conclusions

In the current study, the common stiffened plates in the engineering fields of aviation, aerospace and shipbuilding are taken as the object. Aiming at the geometric distortion of the similarity analysis for stiffened plates, the geometric distortion similarity laws of the stiffened plates in the same direction and the different direction are derived, respectively. The validity of the geometric distortion similarity law is verified through the numerical model of mass-impacted stiffened plate. The main conclusions of this study can be summarized as follows:

- (1) Based on the concept of relative plastic capacity of stiffeners, this paper creatively puts forward the equivalent technique of relative

Table 9
Scale factor of the hetero-directional geometric distortion model.

Model	Geometric dimension and impact load						Response quantity		
	$\beta_L = \beta_h$	$\beta_H \neq \beta_L$	$\beta_b \neq \beta_L$	β_G	β_t	β_V	β_{E_K}	β_δ	β_F
Prototype	1	1	1	1	1	1	1	1	1
Distortion model I	0.1	0.12	0.144	0.0012	0.1	1.2	0.0017	0.12	0.0144
Distortion model II	0.1	0.15	0.225	0.0015	0.1	1.5	0.0034	0.15	0.0225
Distortion model III	0.1	0.18	0.324	0.0018	0.1	1.8	0.0058	0.18	0.0324
Distortion model IV	0.1	0.20	0.400	0.0020	0.1	2.0	0.0080	0.20	0.0400

Table 10
Scale factor of the three distorted models.

Model	Distortion model V			Distortion model VI				Distortion model VII				
	β_H	β_h	β_b	β_H	β_{h_x}	β_{b_x}	β_{a_x}	β_H	β_h	β_b	β_a	$\beta_{(\sigma_d)_b}$
Adjusted scale factors	0.2	0.15	0.178	0.2	0.1	0.53	0.13	0.2	0.1	0.2	0.1	2.0
Unadjusted scale factors	$\beta_G \beta_t \beta_v \beta_{E_K} \beta_\delta$			$\beta_{h_y} \beta_{b_y} \beta_{a_y} \beta_G \beta_t \beta_v$				$\beta_G \beta_t \beta_v \beta_{E_K} \beta_\delta \beta_F$				
	β_F			$\beta_{E_K} \beta_\delta \beta_F$								

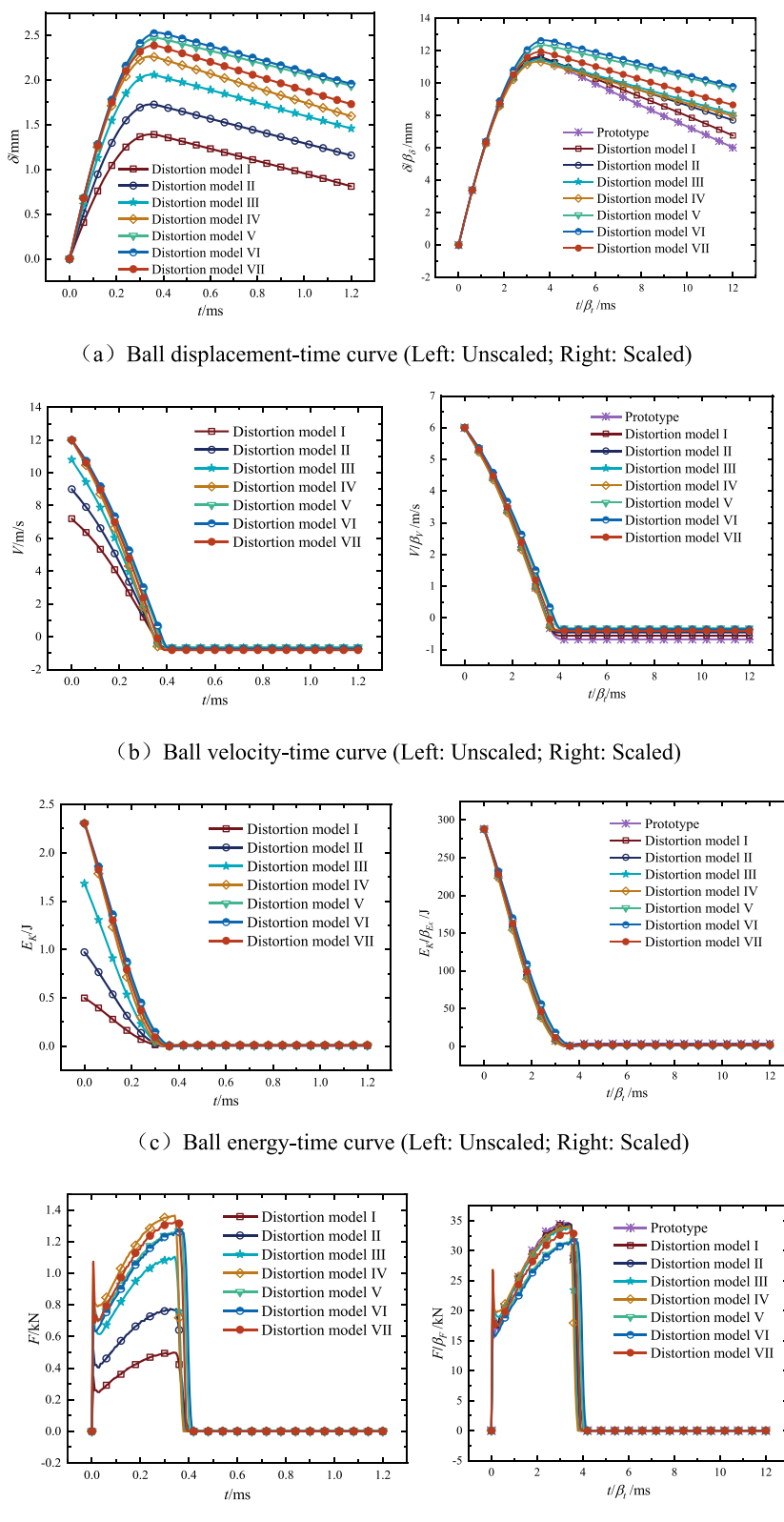


Fig. 9. Dynamic variable-time response curve of prototype and scaled model.

plastic capacity equivalence, in which the equivalent thickness depends on both the thickness of the stiffened plate and the dimensions of stiffeners. From the numerical simulation, it is concluded that the equivalent technique of relative plastic

capacity equivalence is the optimal technique for stiffened plate. In the subsequent study of the similarity for stiffened plates, the equivalent analysis of stiffened plates is carried out by using this equivalent technique.

Table 11
Similarity error of peak displacement predicted by scaled model.

Model	δ/β_s /mm	Similarity error /%
Prototype	11.5689	/
Distortion model I	11.6085	0.343
Distortion model II	11.5217	0.408
Distortion model III	11.4458	1.064
Distortion model IV	11.3199	2.152
Distortion model V	12.3507	6.758
Distortion model VI	12.6485	9.332
Distortion model VII	11.9346	3.161

- (2) The co-directional geometric distortional similarity law of the stiffened plate under impact loads is proposed, which successfully extends the object of the ODLV system to stiffened plate. According to the numerical results, the ODLV system of correcting for velocity, density, and yield stress is still valid for co-directional geometric distortion in the stiffened plate. Moreover, the corrected yield stress and density show better similarity than the corrected velocity, and in practice, it is recommended to use the corrected yield stress and density as much as possible.
- (3) The similarity law of hetero-directional geometric distortion of the stiffened plate structure is derived under the premise that the relative plastic capacity K of the stiffener is constant between scaled model and the prototype. The numerical results show that the scaled model is able to accurately predict the dynamic impact response of the prototype even if the degree of geometric distortion η_H is 2.0, with a similarity error of no more than 3 % in the displacement response. And even under the same degree of geometric distortion, the similarity obtained through co-direction geometric distortion similarity law is inferior to that achieved through hetero-direction geometric distortion similarity law.
- (4) In addition, the control of the width scale factor β_b of the stiffened plate is successfully implemented by three distortion schemes: the simultaneous distortion of the thickness of the stiffened plate, the height and width of the stiffeners; the adjustment of the number of stiffeners along x and y directions in the plane; and the adjustment of the material of the stiffeners. And among them, the similarity error of adjusting the material parameters of stiffeners is the minimum. Consequently, in order to avoid an excessive

degree of distortion in the width of stiffeners, it is recommended to employ this method as much as possible for the scaled models of stiffened plates.

Since the proposed similarity law of geometric distortion for stiffened plates in this study is limited to rigid-perfectly plastic materials, it is necessary to further study the more complex impact problem of stiffened plates considering the effect of elastic deformation. In addition, it is also necessary for future work to design falling weight impact experiments to verify the validity of the similarity law.

CRediT authorship contribution statement

Xinzhe Chang: Writing – original draft, Validation, Software, Methodology, Investigation, Conceptualization. **Fei Xu:** Writing – review & editing, Supervision, Resources, Methodology, Funding acquisition, Conceptualization. **Wei Feng:** Writing – review & editing, Validation. **Xiaocheng Li:** Validation. **Xiaochuan Liu:** Validation.

Declaration of competing interest

The authors declare that they have no known competing financial interests or personal relationships that could have appeared to influence the work reported in this paper.

Data availability

The authors do not have permission to share data.

Acknowledgements

This present paper is supported by the National Natural Science Foundation of China [grant no. 12272320], the National Natural Science Foundation for Young Scientists of China [grant no. 12202336], the China Scholarship Council (CSC) [grant no. 202306290206], the Fundamental Research Funds for the Central Universities (grant no. D5000230141) and the Overseas Expertise Introduction Project for Discipline Innovation (the 111 Project) [grant no. BP0719007].

Appendix A

In order to obtain proper mesh element dimensions, 1 mm, 3 mm and 5 mm mesh element dimensions are selected for numerical analyses, respectively. Comparing the displacement-time and velocity-time curves of different dimensions, as shown in Fig. A1, it is found that the numerical results of 1 mm and 3 mm mesh dimensions are close to each other, which indicates that the results tend to be stable. Therefore, in view of the computational efficiency and accuracy, the 3 mm mesh dimensions are finally selected for numerical analysis.

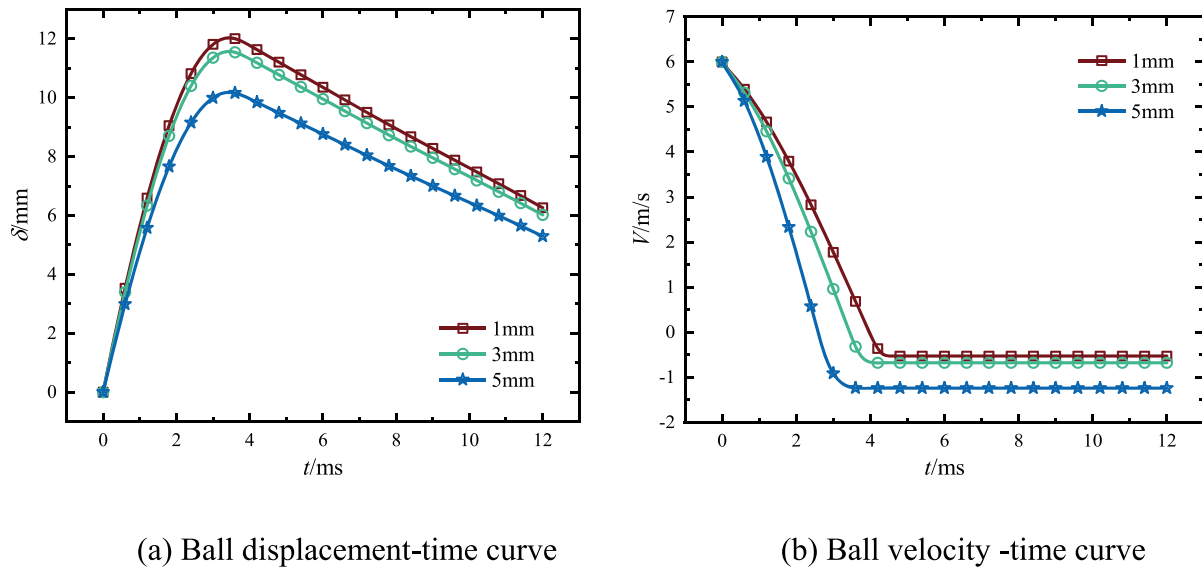
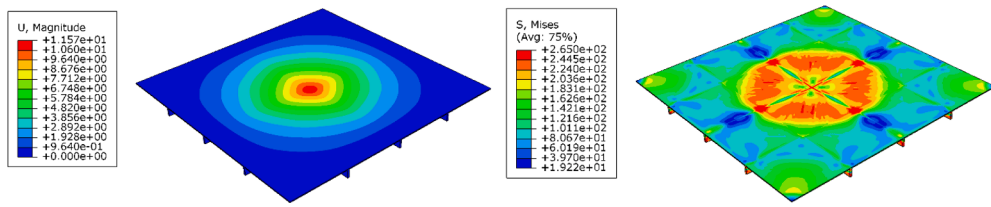


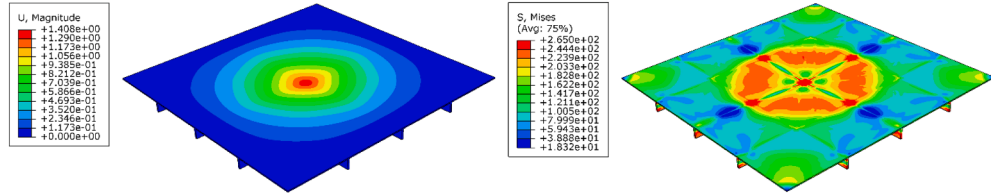
Fig. A1. Dynamic variable-time response curve of different mesh dimensions.

Appendix B

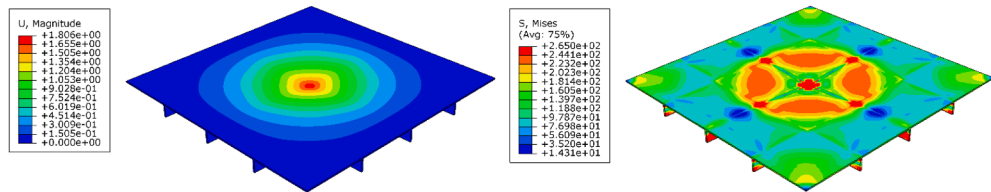
Fig. B1 presents the distribution of deformation and von Mises stress for the prototype and co-directional geometric distortion scaled models, where the distribution of deformation is obtained from the moment of maximum deformation and the distribution of stress is obtained from the final moment.



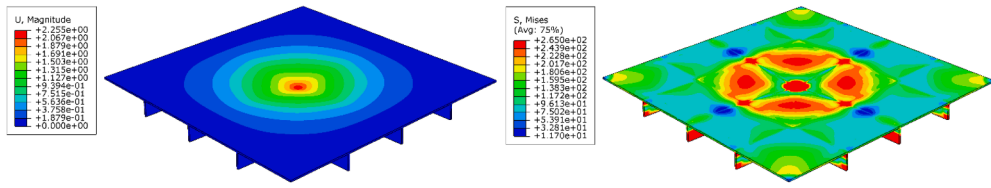
(a) Prototype (Left: Distribution of deformation; Right: Distribution of stress)



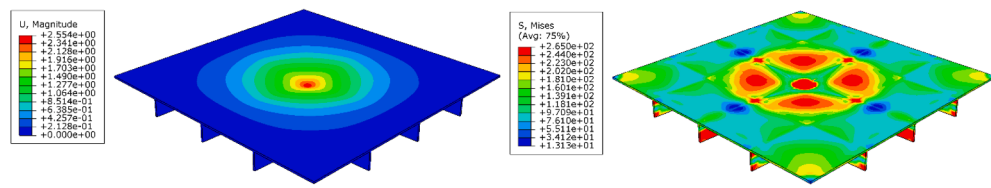
(b) Distortion model I (Left: Distribution of deformation; Right: Distribution of stress)



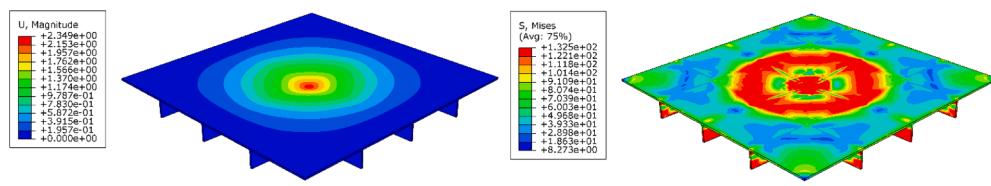
(c) Distortion model II (Left: Distribution of deformation; Right: Distribution of stress)



(d) Distortion model III (Left: Distribution of deformation; Right: Distribution of stress)



(e) Distortion model IV (Left: Distribution of deformation; Right: Distribution of stress)



(f) Distortion model V (Left: Distribution of deformation; Right: Distribution of stress)

Fig. B1. Distribution of deformation and stress.

Fig. B2 presents the distribution of deformation and von Mises stress for the prototype and hetero-directional geometric distortion scaled models, where the distribution of deformation is obtained from the moment of maximum deformation and the distribution of stress is obtained from the final moment.

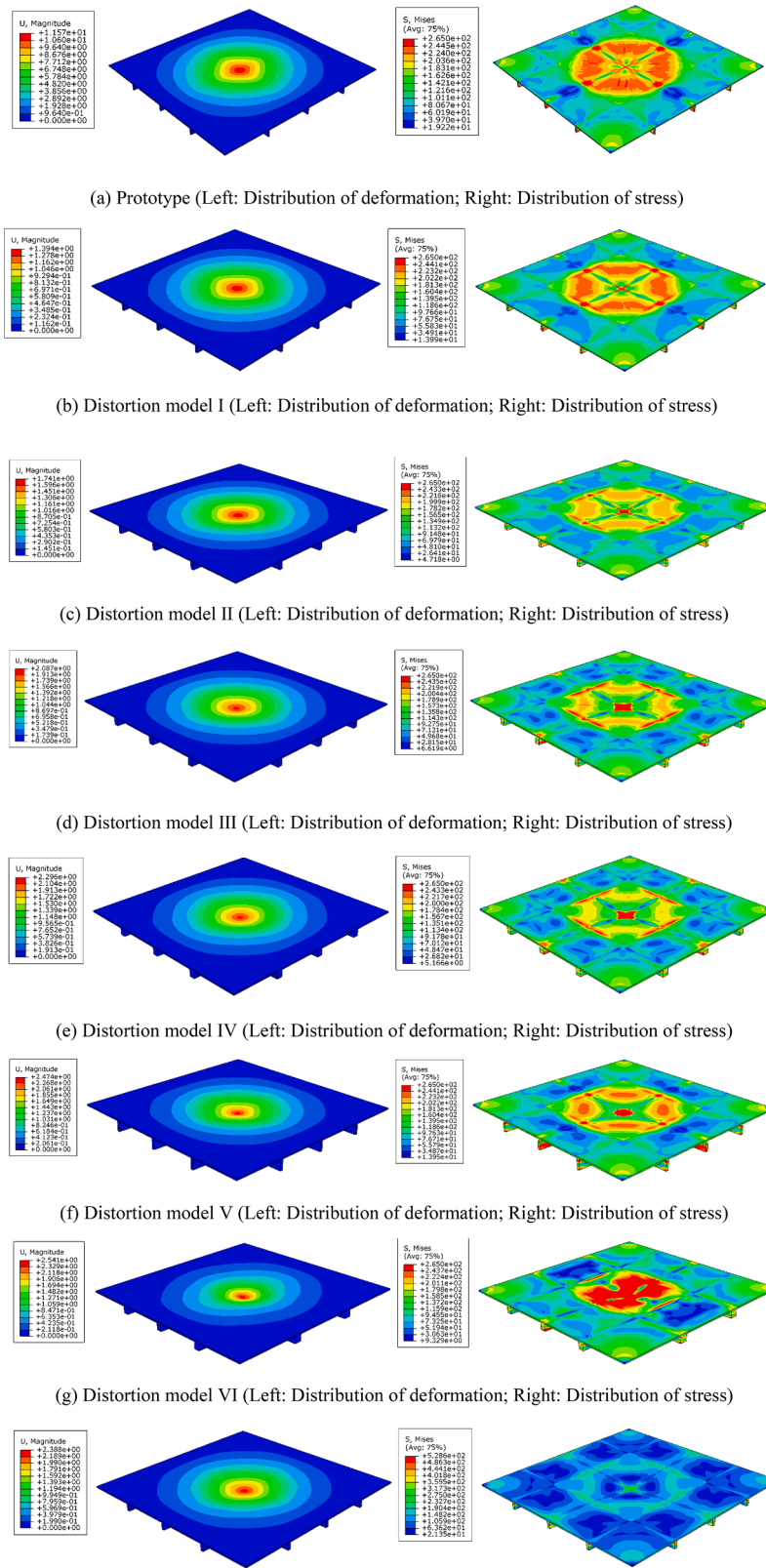


Fig. B2. Distribution of deformation and stress.

References

- [1] B. Zhang, H.J. Wang, Z.H. Qi, et al., Multi-level dynamic responses of blast-loaded orthogrid stiffened panels, *Thin-Walled Struct.* 193 (2023) 111241, <https://doi.org/10.1016/j.tws.2023.111241>.
- [2] L. Ke, K. Liu, Y.Y. Sha, et al., Blast responses of steel stiffened panels subjected to plane shock waves, *Thin-Walled Struct.* 166 (2021) 107933, [10.1016/j.tws.2021.107933](https://doi.org/10.1016/j.tws.2021.107933).
- [3] X.S. Kong, Y. Yang, J. Gan, et al., Experimental and numerical investigation on the detailed buckling process of similar stiffened panels subjected to in-plane compressive load, *Thin-Walled Struct.* 148 (2020) 106620, <https://doi.org/10.1016/j.tws.2020.106620>.
- [4] X. Qin, Y.J. Shen, W. Chen, et al., Bending and free vibration analyses of circular stiffened plates using the FSDT mesh-free method, *Int. J. Mech. Sci.* 202–203 (2021) 106498, <https://doi.org/10.1016/j.ijmecsci.2021.106498>.
- [5] Y.J. Shen, X.C. He, W. Chen, et al., Meshless simulation and experimental study on forced vibration of rectangular stiffened plate, *J. Sound Vib.* 518 (2022) 116602, <https://doi.org/10.1016/j.jsv.2021.116602>.
- [6] J.Z. Liu, Q.G. Fei, D. Jiang, et al., Experimental and numerical investigation on static and dynamic characteristics for curvilinearly stiffened plates using DST-BK model, *Int. J. Mech. Sci.* 169 (2020) 105286, <https://doi.org/10.1016/j.ijmecsci.2019.105286>.
- [7] S. Wang, X.Z. Chang, F. Xu, et al., Similarity laws of geometric and material distortion for anisotropic elastic plate subjected to impact loads, *Int. J. Impact Eng.* 180 (2023) 104683, <https://doi.org/10.1016/j.ijimpeng.2023.104683>.
- [8] C.P. Coutinho, A.J. Baptista, J.Dias Rodrigues, Reduced scale models based on similitude theory: A review up to 2015, *Eng. Struct.* 119 (2016) 81–94, <https://doi.org/10.1016/j.engstruct.2016.04.016>.
- [9] C.P. Coutinho, A.J. Baptista, J.Dias Rodrigues, Modular approach to structural similitude, *Int. J. Mech. Sci.* 135 (2018) 294–312, <https://doi.org/10.1016/j.ijmecsci.2017.11.005>.
- [10] A. Casaburo, G. Petrone, F. Franco, et al., A review of similitude methods for structural engineering, *Appl. Mech. Rev.* 71 (2019) 1–32, <https://doi.org/10.1115/1.4043787>.
- [11] N. Jones, *Structural impact, second ed*, Cambridge University Press, New York, 2012.
- [12] S. Wang, F. Xu, X.Y. Zhang, et al., A directional framework of similarity laws for geometrically distorted structures subjected to impact loads, *Int. J. Impact Eng.* 161 (2022) 104092, <https://doi.org/10.1016/j.ijimpeng.2021.104092>.
- [13] Y.Z. Qin, Y. Wang, Z. Wang, et al., Investigation on similarity laws of cabin structure under internal blast loading, *Ocean Eng.* 260 (2022) 111998, <https://doi.org/10.1016/j.oceaneng.2022.111998>.
- [14] Y.W.Z. Wang, X.L. Yao, et al., Material similarity law of blunt projectiles penetrating scaled steel target plates, *Int. J. Impact Eng.* 178 (2023) 104603, <https://doi.org/10.1016/j.ijimpeng.2023.104603>.
- [15] T. Wang, L. Ni, T. Wu, Dynamic similitude technique for predicting the behaviour of structures subjected to impact loads, *Int. J. Impact Eng.* 163 (2022) 104160, <https://doi.org/10.1016/j.ijimpeng.2022.104160>.
- [16] R.E. Oshiro, M. Alves, Scaling impacted structures, *Arch. Appl. Mech.* 74 (2004) 130–145, <https://doi.org/10.1007/s00419-004-0343-8>.
- [17] M. Alves, R.E. Oshiro, Scaling the impact of a mass on a structure, *Int. J. Impact Eng.* 32 (2006) 1158–1173, <https://doi.org/10.1016/j.ijimpeng.2004.09.009>.
- [18] H. Sadeghi, K. Davey, R. Darvizeh, et al., A scaled framework for strain rate sensitive structures subjected to high rate impact loading, *Int. J. Impact Eng.* 125 (2019) 229–245, <https://doi.org/10.1016/j.ijimpeng.2018.11.008>.
- [19] H. Sadeghi, K. Davey, R. Darvizeh, et al., An investigation into finite similitude for high-rate loading processes: advantages in comparison to dimensional analysis and its practical implementation, *Int. J. Impact Eng.* 140 (2020) 103554, <https://doi.org/10.1016/j.ijimpeng.2020.103554>.
- [20] H. Sadeghi, M. Alitavoli, A. Darvizeh, et al., Dynamic plastic behaviour of strain rate sensitive tubes under axial impact, *Thin-Walled Struct.* 143 (2019) 106220, [10.1016/j.tws.2019.106220](https://doi.org/10.1016/j.tws.2019.106220).
- [21] M. Alves, R.E. Oshiro, Scaling impacted structures when the prototype and the model are made of different materials, *Int. J. Solids Struct.* 43 (2006) 2744–2760, <https://doi.org/10.1016/j.ijsolstr.2005.03.003>.
- [22] L.M. Mazzariol, R.E. Oshiro, M. Alves, A method to represent impacted structures using scaled models made of different materials, *Int. J. Impact Eng.* 90 (2016) 81–94, <https://doi.org/10.1016/j.ijimpeng.2015.11.018>.
- [23] L.M. Mazzariol, M. Alves, Experimental study on scaling of circular tubes subjected to dynamic axial crushing using models of different materials, in: Proceedings of the 22nd International Congress of Mechanical Engineering, Ribeirão Preto, Brazil, 2013, <https://doi.org/10.13140/2.1.312.8967> (COBEM 2013).
- [24] S. Wang, F. Xu, Z. Dai, Suggestion of the DLV dimensionless number system to represent the scaled behavior of structures under impact loads, *Arch. Appl. Mech.* 90 (2020) 707–719, <https://doi.org/10.1007/s00419-019-01635-9>.
- [25] S. Wang, F. Xu, X.Y. Zhang, et al., Material similarity of scaled models, *Int. J. Impact Eng.* 156 (2021) 103951, <https://doi.org/10.1016/j.ijimpeng.2021.103951>.
- [26] L.F. Yang, X.Z. Chang, F. Xu, et al., Study on the scaling law of geometrically-distorted thin-walled cylindrical shells subjected to axial impact, *Explos. Shock Waves.* 42 (2022) 102–113, <https://doi.org/10.11883/bzycj-2021-0452>.
- [27] X.Z. Chang, F. Xu, L.F. Yang, et al., Study on the similarity of axial crushing of thin-walled square tubes, *J. Vib. Shock.* 42 (2023) 284–294, <https://doi.org/10.13465/j.cnki.jvs.2023.11.034>.
- [28] L.L. Zhou, A new structural similitude method for laminated composite cylinders, *Thin-Walled Struct.* 164 (2021) 107920, <https://doi.org/10.1016/j.tws.2021.107920>.
- [29] K. Davey, R. Darvizeh, A. Golbaf, et al., The breaking of geometric similitude, *Int. J. Mech. Sci.* 187 (2020) 105925, <https://doi.org/10.1016/j.ijmecsci.2020.105925>.
- [30] U. Cho, A.J. Dutson, K.L. Wood, et al., An advanced method to correlate scale models with distorted configurations, *J. Mech. Des.* 127 (2005) 78–85, <https://doi.org/10.1115/1.1825044>.
- [31] R.E. Oshiro, M. Alves, Predicting the behaviour of structures under impact loads using geometrically distorted scaled models, *J. Mech. Phys. Solids.* 60 (2012) 1330–1349, <https://doi.org/10.1016/j.jmps.2012.03.005>.
- [32] X.S. Kong, X. Li, C. Zheng, et al., Similarity considerations for scale-down model versus prototype on impact response of plates under blast loads, *Int. J. Impact Eng.* 101 (2017) 32–41, <https://doi.org/10.1016/j.ijimpeng.2016.11.006>.
- [33] L.M. Mazzariol, M. Alves, Similarity laws of structures under impact load: Geometric and material distortion, *Int. J. Mech. Sci.* 157–158 (2019) 633–647, <https://doi.org/10.1016/j.ijmecsci.2019.05.011>.
- [34] Z. Wang, X.S. Kong, W.G. Wu, Corrected similitude method for designing scaled-down stiffened plate subjected to compression load with improved processing feasibility, *Thin-Walled Struct.* 192 (2023) 111201, [10.1016/j.tws.2023.111201](https://doi.org/10.1016/j.tws.2023.111201).
- [35] Q.H. Wang, P.Y. Wei, C.T. Li, et al., A unified similarity criterion and design method for geometrically distorted scale models of thin-walled hull girder structures, *Thin-Walled Struct.* 180 (2022) 109866, [10.1016/j.tws.2022.109866](https://doi.org/10.1016/j.tws.2022.109866).
- [36] Z. Wang, T. Yuan, X.S. Kong, et al., A universal similitude method and design procedure for buckling assessment of stiffened plates under compression load on real ships, *Thin-Walled Struct.* 181 (2022) 110025, [10.1016/j.tws.2022.110025](https://doi.org/10.1016/j.tws.2022.110025).
- [37] T. Yuan, Y. Yang, X.S. Kong, et al., Similarity criteria for the buckling process of stiffened plates subjected to compressive load, *Thin-Walled Struct.* 158 (2021) 107183, [10.1016/j.tws.2020.107183](https://doi.org/10.1016/j.tws.2020.107183).
- [38] M.C. Xu, Z.J. Song, J. Pan, Study on the similarity methods for the assessment of ultimate strength of stiffened panels under axial load based on tests and numerical simulations, *Ocean Eng.* 219 (2021) 108294, <https://doi.org/10.1016/j.oceaneng.2020.108294>.
- [39] X.S. Kong, H. Zhou, Z. Kuang, et al., Corrected method for scaling the dynamic response of stiffened plate subjected to blast load, *Thin-Walled Struct.* 159 (2021) 107214, <https://doi.org/10.1016/j.tws.2020.107214>.
- [40] H.Y. Zhou, D.Y. Wang, Corrected similarity laws of stiffened panels considering geometric distortion under low speed impact load, *Ocean Eng.* 240 (2021) 109937, <https://doi.org/10.1016/j.oceaneng.2021.109937>.
- [41] H. Kenan, C.O. Azeloglu, Design of scaled down model of a tower crane mast by using similitude theory, *Eng. Struct.* 220 (2020) 110985, <https://doi.org/10.1016/j.engstruct.2020.110985>.
- [42] W. Johnson, *Impact strength of materials*, Edward Arnold, London, 1972.
- [43] W. Johnson, A.K. Sengupta, S.K. Ghosh, et al., Mechanics of high-speed impact at normal incidence between plasticine long rods and plates, *J. Mech. Phys. Solids.* 5–6 (1981) 413–445, [https://doi.org/10.1016/0022-5096\(81\)90037-5](https://doi.org/10.1016/0022-5096(81)90037-5).
- [44] Y.P. Zhao, Suggestion of a new dimensionless number for dynamic plastic response of beams and plates, *Arch. Appl. Mech.* 68 (1998) 524–538, <https://doi.org/10.1007/s00419-00050184>.
- [45] Y.P. Zhao, Similarity consideration of structural bifurcation buckling, *Fortsch. Ingenieurwes.* 65 (1999) 107–112, <https://doi.org/10.1007/PL00010868>.
- [46] M.P. Nemeth, A treatise on equivalent-plate stiffnesses for stiffened laminated-composite plates and plate-like lattices, *NASA TP-2011-216882* (2011).
- [47] P. Fu, H.Y. Fan, J.L. Mu, Calculation method of deformation deflection of stiffened plate under underwater explosion, *Jiangsu Ship* 31 (2014) 10–11, <https://doi.org/10.19646/j.cnki.32-1230.2014.03.004>. +34.
- [48] H. Qin, L. Zhou, B. Zhou, Influence of simplified method of stiffened plate on whole vibration of ship hull, *Ship Eng.* 42 (2020) 46–50, <https://doi.org/10.13788/j.cnki.cbcg.2020.11.09>.
- [49] L.Q. Jiao, H.L. Hou, P.Y. Chen, et al., Research on dynamic response and damage characteristics of fixed supported one-way stiffened plates under blast loading, *Acta Armamentariorum* 40 (2019) 592–600, <https://doi.org/10.3969/j.issn.1000-1093.2019.03.019>.
- [50] L. Gan, Z.H. Zong, J. Lin, et al., Damage mechanism of U-shaped ribs stiffened steel flat plates subjected to close-in explosion, *Thin-Walled Struct.* 179 (2022) 109656, <https://doi.org/10.1016/j.tws.2022.109656>.
- [51] H. Wu, W.C. Xu, D.B. Shan, et al., Mechanism of increasing spinnability by multi-pass spinning forming – Analysis of damage evolution using a modified GTN model, *Int. J. Mech. Sci.* 159 (2019) 1–19, <https://doi.org/10.1016/j.ijmecsci.2019.05.030>.
- [52] Y.X. Wang, D.L. Liang, X.L. Xi, et al., Prediction techniques for the scaled models made of different materials under impact loading, *Int. J. Impact Eng.* 179 (2023) 104642, <https://doi.org/10.1016/j.ijimpeng.2023.104642>.
- [53] H.L. Hou, X. Zhu, M.B. Gu, Study on failure mode of stiffened plate and optimized design of structure subjected to blast load, *Explos. Shock Waves.* 27 (2007) 26–33, [https://doi.org/10.11883/1001-1455\(2007\)01-0026-08](https://doi.org/10.11883/1001-1455(2007)01-0026-08).
- [54] S. Cheng, W.X. Liu, N.X. Tong, et al., Damage mechanism of typical stiffened aircraft structures under explosive loading, *Explos. Shock Waves.* 41 (2021) 88–95, <https://doi.org/10.11883/bzycj-2020-0077>.
- [55] N.K. Gupta, Pawan Kumar, S. Hegde, On deformation and tearing of stiffened and un-stiffened square plates subjected to underwater explosion—a numerical study, *Int. J. Mech. Sci.* 52 (2010) 733–744, <https://doi.org/10.1016/j.ijmecsci.2010.01.005>.
- [56] N. Zhao, S.J. Yao, D. Zhang, et al., Experimental and numerical studies on the dynamic response of stiffened plates under confined blast loads, *Thin-Walled Struct.* 154 (2020) 106839, [10.1016/j.tws.2020.106839](https://doi.org/10.1016/j.tws.2020.106839).

- [57] G.N. Nurick, M.E. Gelman, N.S. Marshall, Tearing of blast loaded plates with clamped boundary conditions, *Int. J. Impact Eng.* 18 (1996) 803–827, [https://doi.org/10.1016/S0734-743X\(96\)00026-7](https://doi.org/10.1016/S0734-743X(96)00026-7).
- [58] G.N. Nurick, M.D. Olson, J.R. Fagnan, et al., Deformation and tearing of blast-loaded stiffened square plates, *Int. J. Impact Eng.* 16 (1995) 273–291, [https://doi.org/10.1016/0734-743X\(94\)00046-Y](https://doi.org/10.1016/0734-743X(94)00046-Y).
- [59] S. Wang, F. Xu, Z. Dai, et al., A direct scaling method for the distortion problems of structural impact, *Chin. J. Theor. Appl. Mech.* 52 (2020) 774–786, <https://doi.org/10.6052/0459-1879-19-327>.